



HAL
open science

Mammal Hyaluronidase Activity on Chondroitin Sulfate and Dermatan Sulfate: Mass Spectrometry Analysis of Oligosaccharide Products

Mélanie Bilong, Parisa Bayat, Matthieu Bourderieux, Murielle Jérôme,
Alexandre Giuliani, Régis Daniel

► **To cite this version:**

Mélanie Bilong, Parisa Bayat, Matthieu Bourderieux, Murielle Jérôme, Alexandre Giuliani, et al.. Mammal Hyaluronidase Activity on Chondroitin Sulfate and Dermatan Sulfate: Mass Spectrometry Analysis of Oligosaccharide Products. *Glycobiology*, 2021, 31 (7), pp.751-761. 10.1093/glycob/cwab004 . hal-03103354

HAL Id: hal-03103354

<https://univ-evry.hal.science/hal-03103354>

Submitted on 27 Nov 2021

HAL is a multi-disciplinary open access archive for the deposit and dissemination of scientific research documents, whether they are published or not. The documents may come from teaching and research institutions in France or abroad, or from public or private research centers.

L'archive ouverte pluridisciplinaire **HAL**, est destinée au dépôt et à la diffusion de documents scientifiques de niveau recherche, publiés ou non, émanant des établissements d'enseignement et de recherche français ou étrangers, des laboratoires publics ou privés.

Mammal Hyaluronidase Activity on Chondroitin Sulfate and Dermatan Sulfate: Mass
Spectrometry Analysis of Oligosaccharide Products

Keywords: Chondroitin sulfate / Extreme UV photodissociation / Glycosaminoglycan /
Hyaluronidase

Mélanie Bilong¹, Parisa Bayat¹, Matthieu Bourderioux¹, Murielle Jérôme¹, Alexandre
Giuliani^{2,3}, Régis Daniel^{1*}

¹Université Paris-Saclay, Univ Evry, CNRS, LAMBE, 91025 Evry-Courcouronnes, France

²SOLEIL, l'Orme des Merisiers, St Aubin, BP48, 91192 Gif sur Yvette Cedex, France.

³UAR1008, Transform, INRAe, Rue de la Géraudière, 44316 Nantes, France.

Supplementary Data Included: Figures S1 - S7 and Tables SI – SVII

*Correspondence to: Régis Daniel, Université Paris-Saclay, Univ Evry, Laboratoire Analyse, Modélisation et Matériaux pour la Biologie et l'Environnement, 91025 Evry-Courcouronnes, France, E-mail: regis.daniel@univ-evry.fr.

Abstract

Mammalian hyaluronidases are endo-N-acetyl-D-hexosaminidases involved in the catabolism of hyaluronic acid (HA) but their role in the catabolism of chondroitin sulfate (CS) is also examined. HA and CS are glycosaminoglycans (GAGs) implicated in several physiological and pathological processes, and understanding their metabolism is of significant importance. Data have been previously reported on the degradation of CS under the action of hyaluronidase, yet a detailed structural investigation of CS depolymerization products remains necessary to improve our knowledge of the CS depolymerizing activity of hyaluronidase. For that purpose, the fine structural characterization of CS oligosaccharides formed upon the enzymatic depolymerization of various CS sub-types by hyaluronidase has been carried out by high resolution Orbitrap mass spectrometry and extreme UV (XUV) photodissociation tandem mass spectrometry. The exact mass measurements show the formation of wide size range of even oligosaccharides upon digestion of CS-A and CS-C comprising hexa- and octa-saccharides among the main digestion products, as well as formation of small quantities of odd-numbered oligosaccharides, while no hyaluronidase activity was detected on CS-B. In addition, slight differences have been observed in the distribution of oligosaccharides in the digestion mixture of CS-A and CS-C, the contribution of longer oligosaccharides being significantly higher for CS-C. The sequence of CS oligosaccharide products determined XUV photodissociation experiments verifies the selective $\beta(1\rightarrow4)$ glycosidic bond cleavage catalyzed by mammal hyaluronidase. The ability of the mammal hyaluronidase to produce hexa- and higher oligosaccharides supports its role in the catabolism of CS anchored to membrane proteoglycans and in extra-cellular matrix.

1. Introduction

Defects in the catabolism of glycosaminoglycans (GAGs) and their subsequent accumulation within biological matrices and tissues are associated with several pathological states and diseases. GAGs are a family of linear polysaccharides present on the cell surfaces and in the extracellular matrix, which play important roles in the interaction between cells and matrix, and are involved in a wide variety of biological processes such as cell proliferation, differentiation and migration (Jackson, Busch, and Cardin 1991; Sugahara et al. 2003). The GAGs chondroitin sulfate (CS) and hyaluronic acid (HA) are involved in cartilage pathologies (Schiller et al. 1996). In rheumatic diseases, CS and HA oligosaccharide chains accumulate in synovial fluids causing joint inflammation (Schiller et al. 1996). For this reason and also the implication in other biological processes, understanding their metabolism is of great importance.

CS and HA have distinct catabolism depending on their structure. CS consists of a repeating disaccharide unit of $-4\text{GlcUA}\beta 1-3\text{GalNAc}\beta 1-$ (GlcUA = D-glucuronic acid and GalNAc = *N*-acetyl-D-galactosamine), which can be sulfated at one or multiple positions as follows: *O*-sulfation at C2 on GlcUA, and 4 / 6 positions on GalNAc. Therefore, different combinations of above-mentioned possibilities can occur leading to the following CS families: CS-A (GlcUA- GalNAc(4S)), CS-C (GlcUA-GalNAc(6S)), CS-D (GlcUA(2S)-GalNAc(6S)), CS-E (GlcUA-GalNAc(4S,6S)) and CS-T (GlcUA(2S)-GalNAc(4S,6S)), where 2S, 4S, and 6S represent 2-*O*-, 4-*O*-, and 6-*O*-sulfations, respectively (Farrugia et al. 2019). In addition to sulfation, epimerization of the C6 carboxyl group converts GlcUA into L-iduronic acid (IdoA) resulting in CS-B (IdoA- GalNAc(4S)) also known as dermatan sulfate (DS). The cellular degradation of CS is known to occur in lysosomes; however its exact mechanisms at early stage of catabolism, which might involve exo/endopolysaccharidases, are still poorly understood. HA consists of a repeating disaccharide unit of $-4\text{GlcUA}\beta 1-3\text{GlcNAc}\beta 1-$

(GlcNAc = *N*-acetyl-D-glucosamine). Unlike CS catabolism, the physiological depolymerization of HA is known to be mediated by different hyaluronidase enzymes (EC 3.2.1.35) (Csoka, Frost, and Stern 2001; Meyer and Rapport 1952; Necas et al. 2008; Stern 2003; Wang, Wang, and Li 2017). Given the same β -glycosidic linkages in CS and HA backbones sharing the repeating disaccharide unit $\text{-4Uronic acid}\beta\text{1-3N-Acetylhexosamine}\beta\text{1-}$, the role of the hyaluronidases in CS catabolism has been previously examined (Honda et al. 2012; Yamada 2015). The human hyaluronidase-4 has been shown active *in vivo* on chondroitin sulfate with enzyme activity depending on CS structures (Farrugia et al. 2019; Kaneiwa et al. 2010; Stern and Jedrzejewski 2006; Yamada 2012, 2015).

NMR studies of degradation products from CS and HA in synovial fluid has been previously reported, but the characterization of oligosaccharide structures were difficult due to broad and overlapping signals in NMR spectra (Schiller et al. 1996). Atmospheric pressure ionization mass spectrometry has been employed to monitor the products of the reaction between hyaluronic acid oligosaccharides and bovine testicular hyaluronidase (Takagaki et al. 1994), and MALDI mass spectrometry has been also used to analyze the depolymerization of crude HA and CS by testicular hyaluronidase and to investigate the degradation products of nasal cartilage (Schiller et al. 1999). This later study showed the ability of hyaluronidase to catalyze the depolymerization of CS. However, in absence of tandem mass spectrometry (MS/MS), it did not provide an accurate structural determination of the formed CS oligosaccharides. More recently the human hyaluronidase-4 activity on CS have been studied by steric and ion exchange chromatography, showing endopolysaccharidase activity on CS in mammals (Kaneiwa et al. 2010). It showed preferential depolymerization of CS-D, then CS-C and CS-A substrates among the different CS families, as well as regioselectivity of the glycosidic cleavage (Kaneiwa et al. 2010). However, sparse structural data were provided on the sulfated sequences of CS oligosaccharides formed by hyaluronidase.

Advent of electrospray ionization- mass spectrometry (ESI-MS) with maximal conservation of the labile sulfate groups in the gas phase, and also the development of a wide variety of fragmentation techniques (Bayat, Lesage, and Cole 2020; Pepi et al. 2020) fostered significant advancement in the structural elucidation of GAGs (Chi, Amster, and Linhardt 2005; Kubaski et al. 2017; Laremore et al. 2009; Minsky et al. 2018; Naggar, Costello, and Zaia 2004; Solakyildirim 2019; Joseph Zaia 2013). Among various tandem mass spectrometry techniques that have been employed for the analysis of GAGs, collision-induced dissociation (CID) (Ly et al. 2011; J. Zaia, McClellan, and Costello 2001; Joseph Zaia et al. 2003; Joseph Zaia and Costello 2003), infrared multiphoton dissociation (IRMPD) (Leach, Xiao, et al. 2011; Lettow et al. 2020; Schindler et al. 2017; Wolff et al. 2008b), electron detachment dissociation (EDD) (Agyekum et al. 2015; Kailemia et al. 2014; Leach, Xiao, et al. 2011; Leach, Arungundram, et al. 2012; Leach, Ly, et al. 2012; Wolff et al. 2007, 2008b, 2008a), negative electron transfer dissociation (NETD) (Leach et al. 2017; Leach, Wolff, et al. 2011; Wei et al. 2019; Wolff et al. 2010; Wu et al. 2018), and ultraviolet photodissociation (UVPD)(Klein et al. 2019; Racaud et al. 2009) can be mentioned. Recently, extreme UV (XUV) photodissociation tandem mass spectrometry was introduced that allows producing a substantially informative fragmentation pattern compared to the classical tandem mass spectrometry techniques (Ropartz et al. 2014, 2015). In the study herein, we report the fine structural characterization of CS oligosaccharides formed upon the enzyme depolymerization of CS by mammal hyaluronidase (sheep testes, EC 3.2.35) by using ESI-MS and XUV photodissociation without prior derivatization. Size distribution and sulfate patterns were determined, establishing the structure of CS oligosaccharides formed by hyaluronidase and improving our current knowledge about the catabolism of CS by hyaluronidase.

2. Materials and Methods

2.1. Chemicals

The following materials were purchased from Sigma-Aldrich (Saint-Quentin Fallavier, France): chondroitin sulfate CS-A from bovine trachea (C-8529, ~ 70 % purity), CS-C from shark cartilage (C4384, ~90 % purity), dermatan sulfate DS from porcine intestinal mucosa (C-3788, \geq 90 % purity), hyaluronidase (hyaluronate 4-glycanohydrolase 380 u/mg) from sheep testes (H2126), methanol, acetonitrile, acetic acid, formaldehyde (\geq 36%), Alcian blue 8GX and silver nitrate. Ultra-pure water (18.2 M Ω) was obtained from a Milli-Q purification system (Millipore). Rotiphorese 40 % acrylamide/bisacrylamide (29:1) solution was obtained from Roth (Karlsruhe/Germany). Bio-Gel P-10 was purchased from Bio-Rad (Marnes-la-Coquette).

2.2. Depolymerization by mammal hyaluronidase

Enzyme digestion was performed in the reaction buffer 20 mM sodium phosphate, 77 mM NaCl, pH 7, containing chondroitin sulfate/ dermatan sulfate at a concentration adjusted according to the subsequent analytical method. The reaction was initiated by addition of hyaluronidase (Hyal, 1000 u/mL). After overnight incubation at 37°C, digestion was stopped by heating the samples at 95°C for 5 min.

For MS analysis, 25 μ L of 0.8 mg/mL chondroitin sulfate / dermatan sulfate stock solution in water was diluted in 50 μ L reaction buffer. Enzyme digestion was initiated by addition of 20 μ L of Hyal (1000 u/mL). After overnight incubation and stopping reaction by heating, the reaction mixtures were centrifuged at 15000 rpm for 10 min, and supernatants were collected for MS analysis.

For carbohydrate gel electrophoresis, 6 μ g of chondroitin sulfate / dermatan sulfate was mixed with 6 μ L of Hyal. After overnight incubation and stopping reaction by heating at 95°C, 4 μ L

of glycerol (50 %) and 2 μ L of phenol red were added to the reaction mixture.

For size exclusion chromatography, 2.5 mg of chondroitin sulfate / dermatan sulfate was solubilized in 100 μ L of reaction buffer containing 1000 u/mL of Hyal. After overnight incubation at 37°C and stopping reaction by heating, solution was loaded on preparative size exclusion chromatography Biogel column.

2.3. Carbohydrate-polyacrylamide gel electrophoresis

Carbohydrate-polyacrylamide gel electrophoresis (C-PAGE) was performed in polyacrylamide gels (8.3 \times 7.3 cm; thickness = 1 mm) composed of acrylamide:bis-acrylamide in a 100 mM Tris-HCl buffer, pH 7.8 at 6% and 27% for stacking and resolving gels, respectively. The total reaction mixtures (6 μ g of CS/DS, 1 μ L) were loaded into wells. Gels were run in a Mini-PROTEAN® Tetracell system (Bio-Rad) by applying a constant voltage of 250 V for 45 min and using 40 mM Tris, 40 mM acetic acid, pH 7.8 as running buffer. For the sake of sensitive detection, a double staining was performed using Alcian blue and silver nitrate successively, as reported elsewhere (Bodet et al. 2017). At the end of the run, the gel was immersed into Alcian blue solution (0.5 %) with 2 % of acetic acid for 10 min under moderate stirring conditions. The Alcian blue staining solution was then withdrawn, and the gel was immersed in water for at least one hour under stirring until appearance of blue stained bands. The gel was then immersed in silver nitrate solution (0.4 % in water) in complete darkness for 10 min. The gel was then rinsed three times with water before addition of the developing solution composed of 7 g of sodium carbonate and 80 μ L of formaldehyde diluted in 100 mL water. Once new bands appeared, the developing solution was removed and replaced by acetic acid (5 %) to stop the coloration.

2.4. Size exclusion chromatography

Size exclusion chromatography was performed on a Bio-Gel P-10 column (Bio-Rad, Hercules, CA, USA) (85 x 3.5 cm equilibrated with 0.25 M NaCl, and run at 0.35 mL/min.

Fractions were collected every 10 minutes for 24 hours with an ISCO 328 fraction collector. Elution was constantly monitored by UV detection at 210 nm with a Merck L-4000 UV detector (range 0.01, medium response). Eluted material consisted of a graded series of size-uniform oligosaccharides from disaccharide (dp2) to dodecasaccharide (dp12). To ensure size homogeneity, only the top peaks of each fraction were pooled and lyophilized before further processing. Isolated dried fractions were desalted by gel filtration on a Superdex 30 Increase 10/300 GL column (GE Healthcare Life sciences, Velizy-Villacoublay, France) using an Äkta UV-900 (Amersham, Buckinghamshire, United Kingdom) chromatography system. The Superdex 30 column was equilibrated and run with 0.1 mM NaCl, at 1 mL/min, and elution was monitored by UV detection at 214 nm. Desalted saccharides were finally lyophilized and kept at -20°C until further analysis.

2.5. ESI-MS and tandem MS analysis

ESI MS analysis of size exclusion chromatography purified oligosaccharides was performed using a LTQ XL mass spectrometer (Thermo Fisher Scientific, San Jose, CA, USA). Freeze-dried oligosaccharides were solubilized in 250 μ L water/methanol 50/50 v/v and infused at 3 μ L/min flow rate using a syringe pump.

High resolution MS experiments using a LTQ-XL/Orbitrap hybrid instrument (Thermo Fisher Scientific, San Jose, CA, USA) were carried out to analyze the enzyme reaction mixtures. 2 μ L of the digestion solutions were diluted in 1 mL of methanol, and were infused into the electrospray ionization (ESI) source at a flow rate of 3 μ L/min using a syringe pump. Control solutions were prepared containing either only enzyme (spectrum is not shown) or only polysaccharide, (Fig. S3).

The auxiliary, and sweep gas flows were set at 0 (arbitrary unit) and the temperature of the drying gas was set at 275°C. Electrospray voltage was set at 3.8 kV, capillary voltage at -40 V and tube lens offset at -40 V. These ion source conditions have been adjusted in a way to

minimize in-source fragmentation and at the same time to get reasonable ion intensities.

2.6. XUV photodissociation

XUV photodissociation experiments were performed using extreme UV radiation delivered by the DISCO beamline at the SOLEIL synchrotron radiation facility (Saint-Aubin, France). A LTQ XL mass spectrometer (Thermo Fisher Scientific, San Jose, CA, USA) was on-line connected to the end station of the DISCO beamline (Giuliani et al. 2009). A photon shutter was used to synchronize the photon irradiation with precursor ions trapping. The photon energy was set to 18 eV and the irradiation time was set to 1 s. Precursor ions were isolated with an isolation window of 3 u and the normalized collision energy (NCE) was set to zero to have only XUV activation. For collision-induced dissociation (CID) mass spectra (using the same mass spectrometer), the photon irradiation was stopped, and fragmentation was achieved by increasing the NCE. Thermo Xcalibur 3.0.63 software was used for analyzing the spectra.

3. Results and Discussion

3.1. Analysis of CS and DS depolymerization by gel electrophoresis, and size exclusion chromatography

Depolymerization activity of Hyal on chondroitin sulfate (CS-A and CS-C) and dermatan sulfate (DS) was first assessed by carbohydrate- polyacrylamide gel electrophoresis (C-PAGE) (Figure 1). The C-PAGE profiles of the CS-A and CS-C digests revealed the disappearance of the bands corresponding to CS-A and CS-C polysaccharides upon incubation with Hyal, indicating the full depolymerization of these substrates. Several bands with similar profiles for both CS-A and CS-C appeared at lower molecular weight range, which were attributed to oligosaccharides issued from depolymerization. By contrast, the DS digestion mixture showed neither modification of the polysaccharide content nor formation of oligosaccharide products, supporting the lack of activity of Hyal on dermatan sulfate,

consistent with previous studies (Kaneiwa et al. 2010).

Oligosaccharide products were then separated and purified by size exclusion chromatography (SEC). CS-A and CS-C digests yielded similar peak distributions on SEC chromatograms, which were attributed to oligosaccharides ranging from di- to octadeca-saccharides based on column calibration (Fig. S1). By contrast, no such oligosaccharide peaks were detected with DS, and this polysaccharide remained mostly intact as deduced from its detection as a single peak eluted at void volume. Overall, these results from gel electrophoresis and SEC chromatography indicated that compared to dermatan sulfate, chondroitin sulfate is the preferred substrate of Hyal.

3.2. Mass spectrometry analysis of the CS/DS depolymerization products

To get further structural insight into the oligosaccharides formed by Hyal, their analysis was carried out by negative ionization ESI MS. Mass spectra obtained for three example SEC fractions from CS-A and CS-C digests exhibited multi-charged ion pattern corresponding to structures with the repeating units (GlcUA-GalNAcS)_n, ranging mainly from dp4 to dp18 (Fig. S2). It is worth noting that the formed oligosaccharides were saturated, consistent with the hydrolase-type mechanism of Hyal. These results confirmed the depolymerization of chondroitin sulfate, either sulfated on C4 (CS-A) or C6 (CS-C), into even-numbered oligosaccharides.

To achieve a comprehensive structural identification of the enzyme products, the reaction mixtures from chondroitin sulfate and dermatan sulfate digests were also directly analyzed by high-resolution ESI-MS on LTQ Orbitrap. The mass spectra of the CS-A digest showed ion distributions (theoretical and experimental *m/z* values of all the identified ions along with their absolute intensities are reported in Table S1) mainly attributed to (GlcUA-GalNAcS)-based oligosaccharides ranging from dp2 to dp18 (Fig. 2), *i.e.* consistent with SEC result but a larger range than observed by C-PAGE likely due to the lower sensitivity of gel staining.

In order to have a better insight into the formation of CS oligosaccharides by Hyal, the absolute intensities of corresponding ions have been plotted according to their size, taking into account all the charge states for each oligosaccharide (Fig. 2d). Based on this signal quantification, the major decomposition products of CS-A by Hyal are dp4, dp6, dp8, dp10 and dp12 with a marked prevalence of hexasaccharide (dp6), which represented more than 40 % of the detected oligosaccharides. Relative abundances of various oligosaccharides are not totally consistent with their corresponding peak areas in size exclusion chromatogram that is most probably due to the dissimilar ionization and transportation efficiency of different oligosaccharides or space charge effects. The presence of oligosaccharides containing one or two sulfate less than the intact oligosaccharides was also detected in small amount, with their relative abundances increasing with the oligosaccharide size. This observation may be due either to some undersulfated sequences in the polysaccharide substrate, or to the loss of sulfate upon the MS ionization process. It should be mentioned that minor saturated odd-numbered oligosaccharides (dp3, to dp13) were also detected in addition to the even-numbered oligosaccharides, but at lower signal intensity. These odd oligosaccharides could result either from in-source fragmentation of even-numbered oligosaccharides or from the enzyme activity. We assume they resulted from Hyal activity since we observed small peaks interspersed between the major even-numbered oligosaccharide peaks on SEC chromatogram, which likely correspond to odd oligosaccharides. Formation of odd-numbered oligosaccharides from hyaluronan by leech and bovine teste hyaluronidases has been reported recently (He et al. 2020). Unlike even oligosaccharides, they have identical reducing and non-reducing ends, either a GlcUA residue or a GalNAc(4S) residue as determined by high-resolution ESI-Orbitrap analysis, as for example the pentasaccharides GlcUA- GalNAc(4S)- GlcUA- GalNAc(4S)- GlcUA (annotated as GlcUA-dp5 in Fig. 2) and GalNAc(4S)-GlcUA- GalNAc(4S)- GlcUA- GalNAc(4S) (annotated as GalNAc-dp5 in Fig. 2). CS-A odd

oligosaccharides with GalNAc (4S) unit at the reducing and non-reducing ends are more dominant in the spectrum.

Mass spectrum of the CS-C digest exhibited comparable ions species attributed to (GlcUA-GalNAcS)-based oligosaccharides ranging from dp2 to dp20 (Fig. 3, m/z values of all the identified ions along with their absolute intensities are reported in in Table S2). The major formed oligosaccharides are as follows: dp4, dp6, dp8, dp10, dp12, dp14 and dp16. However, their distribution according to signal intensity showed difference with CS-A (Fig. 3). Although dp6 is again the dominant formed oligosaccharide, the contribution of longer oligosaccharides is significantly higher than in CS-A digest. This difference in the size distribution of oligosaccharides produced by Hyal from CS-A and CS-C polysaccharides could be qualitatively observed from their respective mass spectra, but not from their corresponding C-PAGE profiles. As observed in CS-A digest, odd-numbered oligosaccharides of low intensity, and oligosaccharides with sulfate loss were clearly detected in the spectrum of CS-C digest. These results demonstrate that both CS-A and CS-C polysaccharides are substrate of Hyal, albeit with difference in the size distribution of formed oligosaccharides.

The DS / Hyal reaction mixture was also analyzed by ESI-MS despite the lack of oligosaccharides detected by C-PAGE and SEC upon incubation of dermatan sulfate with Hyal. Mass spectrum showed ions of very low intensity, which were attributed to (GlcUA-GalNAcS)-based oligosaccharides ranging in size from dp4 to dp12. (Fig. S4, m/z values of all the identified ions along with their absolute intensities in Table S3). However, a control incubation of pure DS dodecasaccharide with Hyal failed to evidence any oligosaccharide ions on mass spectrum (Fig. S5), suggesting that (GlcUA-GalNAcS)-based oligosaccharides detected in dermatan digest arose from either DS oligosaccharides initially present in DS polysaccharide preparation or from CS contaminant.

It has to be emphasized that direct comparison of the absolute MS intensities of individual

ions between CS digests is not legitimate, because in each digest, different kinds of ions with dissimilar concentrations exist which influences on the ionization efficiency and ion suppression effects. However, the relative intensities of ions in each digest gives reliable information about the enzymatic activity of the Hyal on a given polysaccharide. Based on the high-resolution ESI-MS experiments, it can be concluded that CS-A and CS-C, but not CS-B, are depolymerized by Hyal, but they produced dissimilar distribution of oligosaccharides. At this stage, it must be noted that MS analysis alone cannot ascertain the sequence of formed oligosaccharides, which were determined by tandem MS using XUV activation presented in the next section.

3.3. XUV photodissociation tandem mass spectrometry analysis

Compared to usual collisional dissociation methods, which lead to limited informative fragmentation in carbohydrate analysis, the recently emerged XUV photodissociation appears as an attractive activation technique (Giuliani, Williams, and Green 2018). Indeed, XUV photodissociation applied to the structural characterization of various sugars, has been reported to provide structurally informative cross ring cleavage ions (Ropartz et al. 2014, 2015). XUV photodissociation tandem mass spectrometry of CS oligosaccharides confirmed the greater cross-ring fragmentation obtained in a single MS/MS step as compared to CID experiments in which fragment ions resulted mainly from glycosidic bond cleavages (see CID fragments from the CS-A hexasaccharide ion $[\text{dp6-4H}]^4$ and CS-C octasaccharide ion $[\text{dp8-5H}]^5$ are in Tables S6 and S7 and corresponding mass spectra in Fig. S6 and Fig. S7, respectively). Fig. 4 and Fig. 5 present the XUV fragmentation spectra of CS-A hexasaccharide and CS-C octasaccharide as two representative examples, and their respective cleavage maps for the selected ions $[\text{dp6-4H}]^4$ and $[\text{dp8-5H}]^5$. All the identified fragment ions have been listed in Tables S4 and S5. In the fragment ion map of Fig. 4, cleavages such as $^{3,5}\text{A}_5^{2-}$, $^{1,5}\text{X}_1$, $^{1,5}\text{X}_3^{2-}$, $^{2,5}\text{X}_3^{2-}$, $^{1,5}\text{X}_5^{3-}$ and $^{3,5}\text{X}_5^{3-}$ from CS-A dp6 (plain lines in the cleavage

map Fig. 4, Domon and Costello nomenclature (Domon and Costello 1988)), demonstrate that Hyal cleaves the $\beta(1\rightarrow4)$ linkage, resulting in GlcUA residue at the non-reducing end of the formed oligosaccharide. Similarly, $^{2,4}A_2$, $^{3,5}A_5^{2-}$, $^{3,5}A_7^{3-}$, $^{1,5}X_1$, $^{1,5}X_3^{2-}$, $^{2,5}X_5^{3-}$ and $^{3,5}X_7^{4-}$ cleavages from CS-C dp8 (Fig. 5) confirm the presence of GlcUA at the non-reducing end of the $[dp8-5H]^{5-}$ ion. The specific cleavage of $\beta(1\rightarrow4)$ linkage by Hyal has been previously explained for HA degradation as a result of either the helical structure of HA with exposed $\beta(1\rightarrow4)$ bonds or the larger conformational flexibility of $\beta(1\rightarrow4)$ linkage compared to $\beta(1\rightarrow3)$ bond (Stern and Jedrzejewski 2006). The XUV fragmentation spectra showed preservation of the sulfate groups in fragment ions similarly to UVPD experiments (Klein et al. 2019), which is useful to the determination of the sulfate group location, and consistently indicating sulfation on C4 and C6 of GalNAc residues of oligosaccharides from CS-A and CS-C digests, respectively.

4. Conclusions

In this study we have investigated the activity of the mammal Hyal on chondroitin sulfate polysaccharides. Although the different CS-A and CS-C polysaccharides exhibit similar degradation pattern upon the action of Hyal in C-PAGE and SEC separations, the exact mass measurements by MS analysis showed different distribution of depolymerization products according to the sulfate position, the CS-C (4-*O*-sulfated) digestion mixture containing a higher abundance of longer oligosaccharides such as dp10 and dp12. The ability of Hyal to produce hexa- and higher oligosaccharides makes it a valuable tool for the structural analysis of GAGs. In addition, the exact mass measurements evidenced the formation of odd-numbered oligosaccharides in low amount. No Hyal activity was detected on dermatan sulfate, confirming that the C5 epimerization of the GlcUA into IdoA residue is an obstacle to the activity of hyaluronidase. One can assume that the C5 epimerization alters the recognition

of the uronic residue at the Hyal active site or that it may modify the exposition of the nearby the $\beta(1\rightarrow4)$ glycosidic bond. Finally, XUV photodissociation experiments performed for the first time on glycosaminoglycans, established the sequence and sulfate pattern of CS oligosaccharides formed by Hyal, and extended to the CS polysaccharides family the cleavage specificity of Hyal for the $\beta(1\rightarrow4)$ glycosidic bond. Overall, these results support the role of the secreted mammal Hyal in the early catabolism of CS anchored to membrane proteoglycans and in extra-cellular matrix (Farrugia et al. 2019). Its endopolysaccharidase activity produce CS oligosaccharides of polymerization degree range compatible with subsequent degradation by CS specific exohydrolases and sulfatases in cellular lysosomes.

Acknowledgments

MB acknowledges PhD fellowship from doctoral school SDSV (N°577, Université Paris-Saclay), PB acknowledges post-doctoral fellowship from the program CHARMMMAT ANR-11-LABX-0039-grant supported by the French National Research Agency.

5. References

Agyekum, Isaac et al. 2015. "Assignment of Hexuronic Acid Stereochemistry in Synthetic Heparan Sulfate Tetrasaccharides with 2-O-Sulfo Uronic Acids Using Electron Detachment Dissociation." *International Journal of Mass Spectrometry* 390: 163–69. <http://dx.doi.org/10.1016/j.ijms.2015.08.018>.

Bayat, Parisa, Denis Lesage, and Richard B. Cole. 2020. "Tutorial: Ion Activation in Tandem Mass Spectrometry Using Ultra-High Resolution Instrumentation." *Mass Spectrometry Reviews* 39(5–6): 680–702. <http://dx.doi.org/10.1002/mas.21623>.

Bodet, Pierre Edouard et al. 2017. "Efficient Recovery of Glycosaminoglycan Oligosaccharides from Polyacrylamide Gel Electrophoresis Combined with Mass Spectrometry Analysis." *Analytical and Bioanalytical Chemistry* 409(5): 1257–69. <http://dx.doi.org/10.1007/s00216-016-0052-5>.

Chi, Lianli, Jonathan Amster, and Robert Linhardt. 2005. "Mass Spectrometry for the Analysis of Highly Charged Sulfated Carbohydrates." *Current Analytical Chemistry* 1(3): 223–40.

Csoka, Antonei B., Gregory I. Frost, and Robert Stern. 2001. "The Six Hyaluronidase-like Genes in the Human and Mouse Genomes." *Matrix Biology* 20(8): 499–508.

Domon, Bruno, and Catherine E Costello. 1988. "A Systematic Nomenclature for Carbohydrate Fragmentations in FAB-MS/MS Spectra of Glycoconjugates." *Glycoconjugate Journal* 5(4): 397–409. <http://link.springer.com/10.1007/BF01049915> (July 7, 2017).

Farrugia, Brooke L. et al. 2019. "Hyaluronidase-4 Is Produced by Mast Cells and Can Cleave Serglycin Chondroitin Sulfate Chains into Lower Molecular Weight Forms." *Journal of Biological Chemistry* 294: 11458–72.

Giuliani, Alexandre et al. 2009. "DISCO: A Low-Energy Multipurpose Beamline at Synchrotron SOLEIL." *Journal of Synchrotron Radiation* 16(6): 835–41. <https://onlinelibrary.wiley.com/doi/abs/10.1107/S0909049509034049>.

Giuliani, Alexandre, Jonathan P. Williams, and Martin R. Green. 2018. "Extreme Ultraviolet Radiation: A Means of Ion Activation for Tandem Mass Spectrometry." *Analytical Chemistry* 90(12): 7176–80.

He, Jing et al. 2020. "SI-Construction of Saturated Odd- and Even-Numbered Hyaluronan Oligosaccharide Building Block Library." *Carbohydrate Polymers* 231(86): 1–13. <https://doi.org/10.1016/j.carbpol.2019.115700>.

Honda, Tomoko et al. 2012. "Hyaluronidases Have Strong Hydrolytic Activity toward Chondroitin 4-Sulfate Comparable to That for Hyaluronan." *Biomolecules* 2(4): 549–63.

Jackson, R. L., S. J. Busch, and A. D. Cardin. 1991. "Glycosaminoglycans: Molecular Properties, Protein Interactions, and Role in Physiological Processes." *Physiological Reviews* 71(2): 481–539.

Kailemia, Muchena J et al. 2014. "High-Field Asymmetric-Waveform Ion Mobility Spectrometry and Electron Detachment Dissociation of Isobaric Mixtures of Glycosaminoglycans." *J. Am. Soc. Mass Spectrom.* 25: 258–68.

Kaneiwa, Tomoyuki, Shuji Mizumoto, Kazuyuki Sugahara, and Shuhei Yamada. 2010. "Identification of Human Hyaluronidase-4 as a Novel Chondroitin Sulfate Hydrolase That Preferentially Cleaves the Galactosaminidic Linkage in the Trisulfated Tetrasaccharide Sequence." *Glycobiology* 20(3): 300–309.

Klein, Dustin R., Franklin E. Leach, I. Jonathan Amster, and Jennifer S. Brodbelt. 2019. "Structural Characterization of Glycosaminoglycan Carbohydrates Using Ultraviolet

Photodissociation.” *Analytical Chemistry* 91(9): 6019–26.

Kubaski, Francyne et al. 2017. “Glycosaminoglycans Detection Methods: Applications of Mass Spectrometry.” *Molecular Genetics and Metabolism* 120(1–2): 67–77. <http://dx.doi.org/10.1016/j.ymgme.2016.09.005>.

Laremore, Tatiana N. et al. 2009. “Recent Progress and Applications in Glycosaminoglycan and Heparin Research.” *Current Opinion in Chemical Biology* 13(5–6): 633–40.

Leach, Franklin E., Zhongping Xiao, et al. 2011. “Electron Detachment Dissociation and Infrared Multiphoton Dissociation of Heparin Tetrasaccharides.” *International Journal of Mass Spectrometry* 308(2–3): 253–59.

Leach, Franklin E., Jeremy J. Wolff, et al. 2011. “Negative Electron Transfer Dissociation Fourier Transform Mass Spectrometry of Glycosaminoglycan Carbohydrates.” *European Journal of Mass Spectrometry* 17(2): 167–76. <http://journals.sagepub.com/doi/10.1255/ejms.1120> (March 26, 2020).

Leach, Franklin E., Sailaja Arungundram, et al. 2012. “Electron Detachment Dissociation of Synthetic Heparan Sulfate Glycosaminoglycan Tetrasaccharides Varying in Degree of Sulfation and Hexuronic Acid Stereochemistry.” *International Journal of Mass Spectrometry* 330–332: 152–59. <https://linkinghub.elsevier.com/retrieve/pii/S1387380612002242>.

Leach, Franklin E., Mellisa Ly, et al. 2012. “SI_Hexuronic Acid Stereochemistry Determination in Chondroitin Sulfate Glycosaminoglycan Oligosaccharides by Electron Detachment Dissociation.” *Journal of the American Society for Mass Spectrometry* 23(9): 2–5.

Leach, Franklin E. et al. 2017. “Negative Electron Transfer Dissociation Sequencing of Increasingly Sulfated Glycosaminoglycan Oligosaccharides on an Orbitrap Mass

- Spectrometer.” *Journal of the American Society for Mass Spectrometry* 28(9): 1844–54.
- Lettow, Maike et al. 2020. “IR Action Spectroscopy of Glycosaminoglycan Oligosaccharides.” *Analytical and Bioanalytical Chemistry* 412(3): 533–37.
- Ly, Mellisa et al. 2011. “The Proteoglycan Bikunin Has a Defined Sequence.” *Nature Chemical Biology* 7(11): 827–33.
- Meyer, Karl, and Maurice M Rapport. 1952. 13 Advances in enzymology and related subjects of biochemistry *Hyaluronidases*. United States.
- Minsky, Burcu B. et al. 2018. “Mass Spectrometry Reveals a Multifaceted Role of Glycosaminoglycan Chains in Factor Xa Inactivation by Antithrombin.” *Biochemistry* 57(32): 4880–90.
- Naggar, Estee F., Catherine E. Costello, and Joseph Zaia. 2004. “Competing Fragmentation Processes in Tandem Mass Spectra of Heparin-like Glycosaminoglycans.” *Journal of the American Society for Mass Spectrometry* 15(11): 1534–44.
- Necas, Jiri, L. Bartosikova, P. Brauner, and J. Kolar. 2008. “Hyaluronic Acid (Hyaluronan): A Review.” *Veterinarni Medicina* 53(8): 397–411.
- Pepi, Lauren E., Patience Sanderson, Morgan Stickney, and I. Jonathan Amster. 2020. “Developments in Mass Spectrometry for Glycosaminoglycan Analysis: A Review.” *Molecular & Cellular Proteomics*: mcp.R120.002267.
- Racaud, Amandine et al. 2009. “Wavelength-Tunable Ultraviolet Photodissociation (UVPD) of Heparin-Derived Disaccharides in a Linear Ion Trap.” *Journal of the American Society for Mass Spectrometry* 20(9): 1645–51. <http://dx.doi.org/10.1016/j.jasms.2009.04.022> (July 8, 2019).
- Ropartz, David et al. 2014. “Deciphering the Structure of Isomeric Oligosaccharides in a

Complex Mixture by Tandem Mass Spectrometry: Photon Activation with Vacuum Ultra-Violet Brings Unique Information and Enables Definitive Structure Assignment.” *Analytica Chimica Acta* 807: 84–95.

Ropartz, David et al. 2015. “High-Energy Photon Activation Tandem Mass Spectrometry Provides Unprecedented Insights into the Structure of Highly Sulfated Oligosaccharides Extracted from Macroalgal Cell Walls.” *Analytical Chemistry* 87(2): 1042–49.

Schiller, Jürgen et al. 1999. “Cartilage Degradation by Hyaluronate Lyase and Chondroitin ABC Lyase: A MALDI-TOF Mass Spectrometric Study.” *Carbohydrate Research* 318(1–4): 116–22.

Schiller, Jürgen, Jürgen Arnhold, Kerstin Sonntag, and Klaus Arnold. 1996. “NMR Studies on Human, Pathologically Changed Synovial Fluids: Role of Hypochlorous Acid.” *Magnetic Resonance in Medicine* 35(6): 848–53. <http://doi.wiley.com/10.1002/mrm.1910350610> (April 8, 2020).

Schindler, B. et al. 2017. “IRMPD Spectroscopy Sheds New (Infrared) Light on the Sulfate Pattern of Carbohydrates.” *Journal of Physical Chemistry A* 121(10): 2114–20.

Solakyildirim, Kemal. 2019. “Recent Advances in Glycosaminoglycan Analysis by Various Mass Spectrometry Techniques.” *Analytical and Bioanalytical Chemistry* 411: 3731–3741.

Stern, Robert. 2003. “Devising a Pathway for Hyaluronan Catabolism: Are We There Yet?” *Glycobiology* 13(12): 105–15.

Stern, Robert, and Mark J. Jedrzejas. 2006. “Hyaluronidases: Their Genomics, Structures, and Mechanisms of Action.” *Chemical Reviews* 106(3): 818–39.

Sugahara, Kazuyuki et al. 2003. “Recent Advances in the Structural Biology of Chondroitin Sulfate and Dermatan Sulfate.” *Current Opinion in Structural Biology* 13(5): 612–20.

Takagaki, Keiichi et al. 1994. "Characterization of Hydrolysis and Transglycosylation by Testicular Hyaluronidase Using Ion-Spray Mass Spectrometry." *Biochemistry* 33(21): 6503–7.

Wang, Wenshuang, Junhong Wang, and Fuchuan Li. 2017. "Hyaluronidase and Chondroitinase." In *Advances in Experimental Medicine and Biology*, Springer New York LLC, 75–87.

Wei, Juan et al. 2019. "Characterization and Quantification of Highly Sulfated Glycosaminoglycan Isomers by Gated-Trapped Ion Mobility Spectrometry Negative Electron Transfer Dissociation MS/MS." *Analytical Chemistry* 91(4): 2994–3001.

Wolff, Jeremy J. et al. 2008a. "Electron Detachment Dissociation of Dermatan Sulfate Oligosaccharides." *Journal of the American Society for Mass Spectrometry* 19(2): 294–304. <http://link.springer.com/10.1016/j.jasms.2007.10.007> (July 4, 2019).

Wolff, Jeremy J. et al. 2008b. "Influence of Charge State and Sodium Cationization on the Electron Detachment Dissociation and Infrared Multiphoton Dissociation of Glycosaminoglycan Oligosaccharides." *Journal of the American Society for Mass Spectrometry* 19(6): 790–98.

Wolff, Jeremy J. et al. 2010. "Negative Electron Transfer Dissociation of Glycosaminoglycans." *Analytical Chemistry* 82(9): 3460–66. <https://pubs.acs.org/doi/10.1021/ac100554a> (July 7, 2019).

Wolff, Jeremy J., Lianli Chi, Robert J. Linhardt, and I. Jonathan Amster. 2007. "Distinguishing Glucuronic from Iduronic Acid in Glycosaminoglycan Tetrasaccharides by Using Electron Detachment Dissociation." *Analytical Chemistry* 79(5): 2015–22. <https://pubs-acrs-org.ezproxy.universite-paris-saclay.fr/doi/abs/10.1021/ac061636x> (July 7, 2019).

Wu, Jiandong et al. 2018. “Negative Electron Transfer Dissociation Sequencing of 3-O-Sulfation-Containing Heparan Sulfate Oligosaccharides.” *Journal of the American Society for Mass Spectrometry* 29(6): 1262–72.

Yamada, Shuhei. 2012. “Chondroitin Sulfate-Specific Novel Hydrolase in Human.” In *Advances in Experimental Medicine and Biology*, eds. P. Sudhakaran and A. Surolia. Springer, New York, NY, 47–56.

Yamada, Shuhei. 2015. “Role of Hyaluronidases in the Catabolism of Chondroitin Sulfate.” In *Advances in Experimental Medicine and Biology*, Springer New York LLC, 185–97.

Zaia, J., J. E. McClellan, and C. E. Costello. 2001. “Tandem Mass Spectrometric Determination of the 4S/6S Sulfation Sequence in Chondroitin Sulfate Oligosaccharides.” *Analytical Chemistry* 73(24): 6030–39.

Zaia, Joseph. 2013. “Glycosaminoglycan Glycomics Using Mass Spectrometry.” *Molecular and Cellular Proteomics* 12(4): 885–92.

Zaia, Joseph, and Catherine E. Costello. 2003. “Tandem Mass Spectrometry of Sulfated Heparin-like Glycosaminoglycan Oligosaccharides.” *Analytical Chemistry* 75(10): 2445–55.

Zaia, Joseph, Xue Qing Li, Shiu Yung Chan, and Catherine E. Costello. 2003. “Tandem Mass Spectrometric Strategies for Determination of Sulfation Positions and Uronic Acid Epimerization in Chondroitin Sulfate Oligosaccharides.” *Journal of the American Society for Mass Spectrometry* 14(11): 1270–81.

Figure captions

Fig. 1- C-PAGE profile of intact CS-A, DS and CS-C and their corresponding digests. Digestion was performed by incubation of 6 μg of each individual polysaccharide with 6 μL of 1000 u/mL Hyal at 37°C overnight. 27% polyacrylamide gel electrophoresis, double staining by Alcian blue and silver nitrate.

Fig. 2- Negative ion mode ESI- Orbitrap mass spectrum of the CS-A digest. To have a better view of the observed ions, different regions of the spectrum are separately shown as follows: (a) m/z 250-500, (b) m/z 500-750, and (c) m/z 750-1000 ranges. Ions indicated by red stars have been present in the control solution containing only the enzyme without substrate; ion indicated by a pink star has been present in the control solution containing only the substrate in the absence of the enzyme; no ion was identified in the m/z 750-1000 range (panel (c)). (d) Absolute intensities of the different oligosaccharides observed in the ESI-Orbitrap mass spectrum of the CS-A digest plotted according to their size, taking into account all the charge states for each oligosaccharide. For each individual ion only the intensity of the monoisotopic peak was counted. Digestion was performed by incubation of 0.2 mg of CS-A with 20 μL of Hyal (1000 u/mL) at 37°C overnight. Direct infusion (3 $\mu\text{L}/\text{min}$) of the digestion mixture diluted in methanol.

Fig. 3- Negative ion mode ESI- Orbitrap spectrum of the CS-C digest. To have a better view of the observed ions, different regions of the spectrum are shown separately as follows: (a) m/z 250-500, (b) m/z 500-750, and (c) m/z 750-1000 ranges. Ions indicated by red stars have been present in the control solution containing only the enzyme without substrate. (d) Absolute intensities of different oligosaccharides observed in the ESI-Orbitrap mass spectrum of the CS-C digest plotted according to their size, taking into account all the charge states for each oligosaccharide. For each individual ion only the intensity of the monoisotopic peak was counted. Digestion was performed by incubation of 0.2 mg of CS-C with 20 μL of Hyal (1000 u/mL) at 37°C overnight. Direct infusion (3 $\mu\text{L}/\text{min}$) of the digestion mixture diluted in methanol.

Fig. 4- Extreme-UV photodissociation of hexasaccharide SEC fraction of CS-A digestion mixture. (a) Fragmentation spectrum of the isolated ion $[\text{dp}6\text{-}4\text{H}]^4$ (m/z 347.8) and (b) XUV cleavage map (without indication of the charge state of fragment ions due to space limitation). Cleavages indicated with plain lines demonstrate the sequence with a GlcUA unit at the non-reducing end (GlcUA-GalNAc(4S)- GlcUA- GalNAc(4S)). Identified fragment ions are summarized in Table S4. Digestion conditions as in Fig. 2. Direct infusion (3 $\mu\text{L}/\text{min}$) of the digestion mixture diluted in methanol.

Fig. 5- Extreme-UV photodissociation of octasaccharide SEC fraction of CS-C digestion mixture. (a) Fragmentation spectrum of the isolated ion $[\text{dp}8\text{-}5\text{H}]^5$ (m/z 369.8) and (b) XUV cleavage map (without indication of the charge state of fragment ions due to space limitation). Cleavages indicated with plain lines demonstrate the sequence with a GlcUA unit in the non-reducing end (GlcUA-GalNAc(6S)- GlcUA- GalNAc(6S)- GlcUA- GalNAc(6S)). Identified fragment ions are summarized in Table S5. Digestion conditions as in Fig. 2. Direct infusion (3 $\mu\text{L}/\text{min}$) of the digestion mixture diluted in methanol.

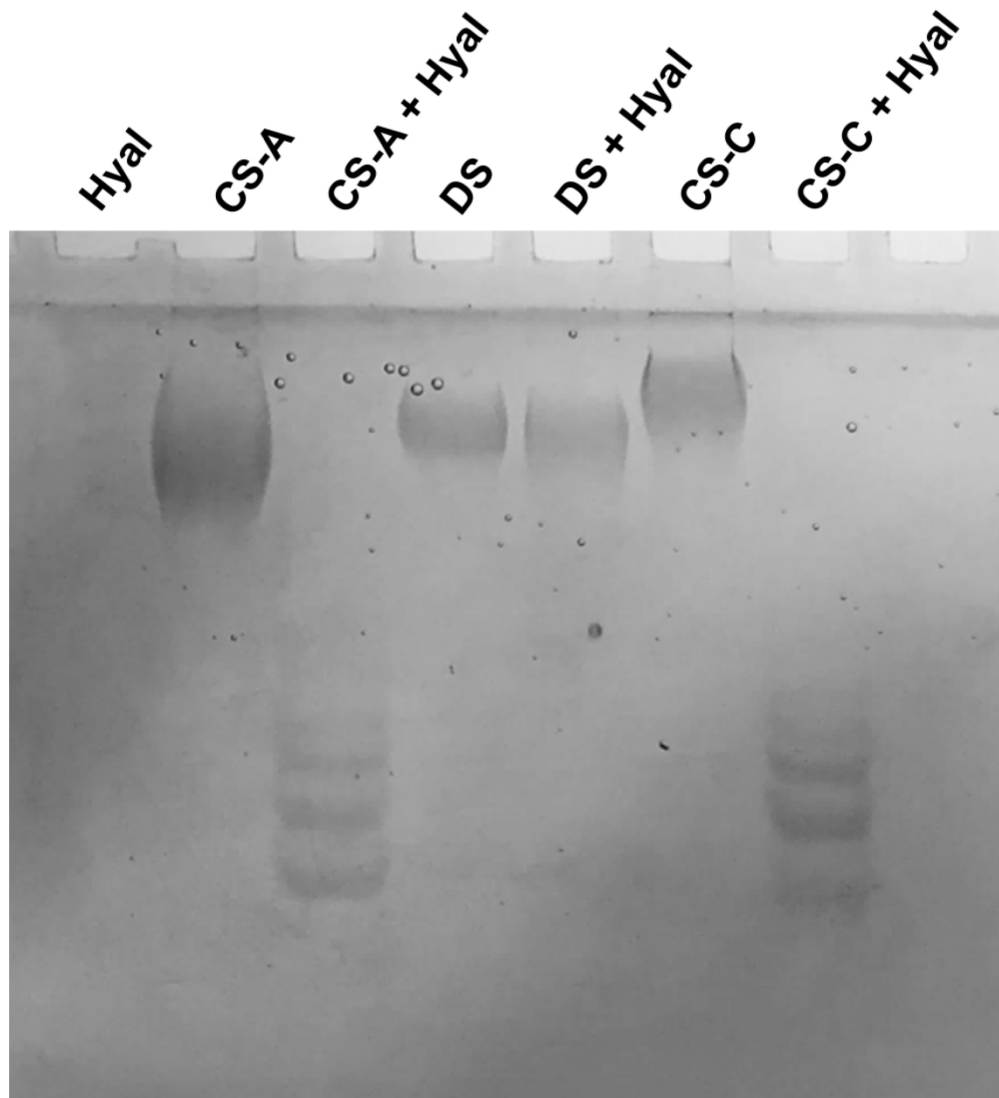


Fig. 1- C-PAGE profile of intact CS-A, DS and CS-C and their corresponding digests. Digestion was performed by incubation of 6 μg of each individual polysaccharide with 6 μL of 1000 u/mL Hyal at 37°C overnight. 27% polyacrylamide gel electrophoresis, double staining by Alcian blue and silver nitrate.

254x290mm (300 x 300 DPI)

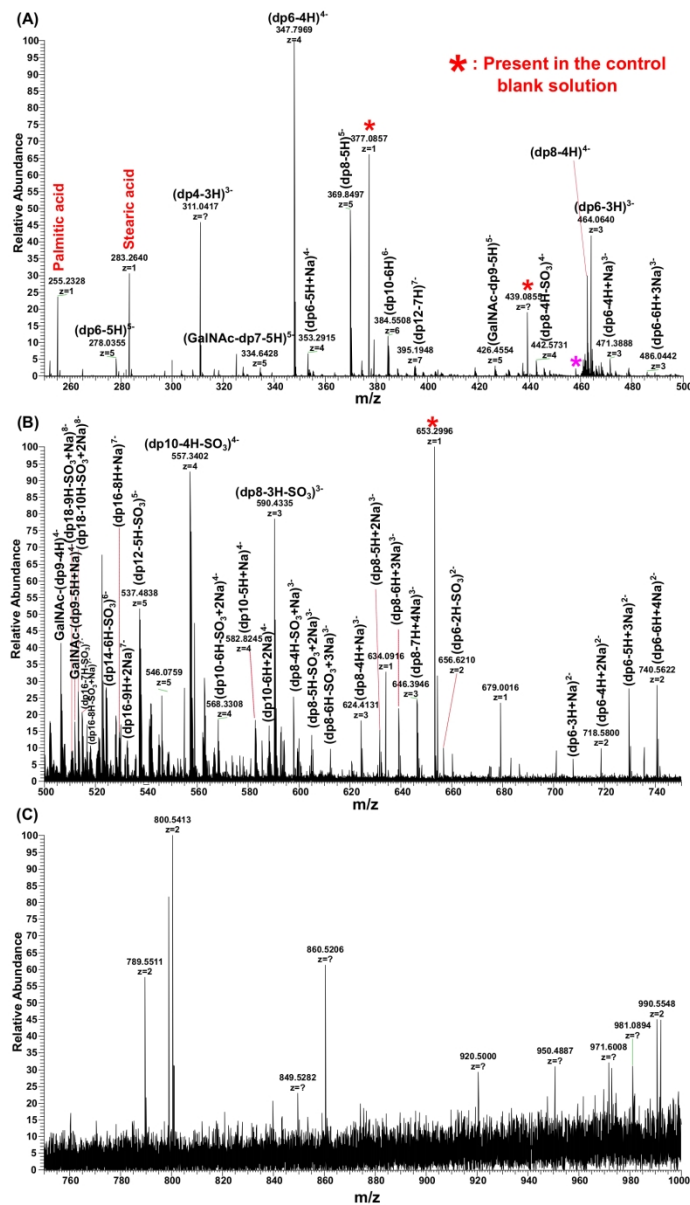
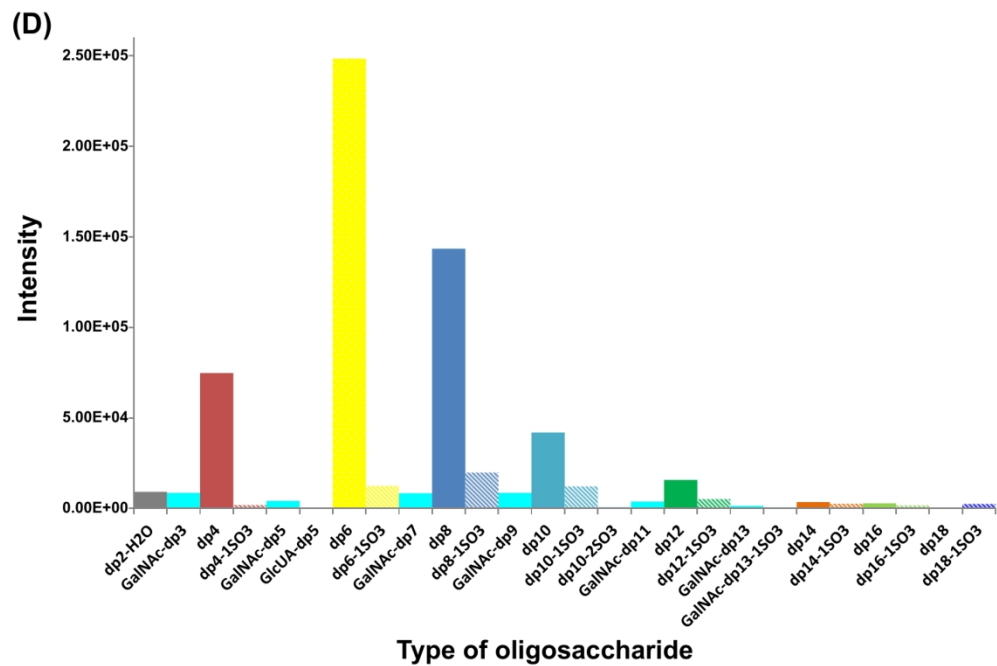


Fig. 2- Negative ion mode ESI- Orbitrap mass spectrum of the CS-A digest. To have a better view of the observed ions, different regions of the spectrum are separately shown as follows: (a) m/z 250-500, (b) m/z 500-750, and (c) m/z 750-1000 ranges. Ions indicated by red stars have been present in the control solution containing only the enzyme without substrate; ion indicated by a pink star has been present in the control solution containing only the substrate in the absence of the enzyme; no ion was identified in the m/z 750-1000 range (panel (c)). (d) Absolute intensities of the different oligosaccharides observed in the ESI-Orbitrap mass spectrum of the CS-A digest plotted according to their size, taking into account all the charge states for each oligosaccharide. For each individual ion only the intensity of the monoisotopic peak was counted. Digestion was performed by incubation of 0.2 mg of CS-A with 20 μ L of Hyal (1000 u/mL) at 37°C overnight. Direct infusion (3 μ L/min) of the digestion mixture diluted in methanol.

413x719mm (600 x 600 DPI)



476x317mm (300 x 300 DPI)

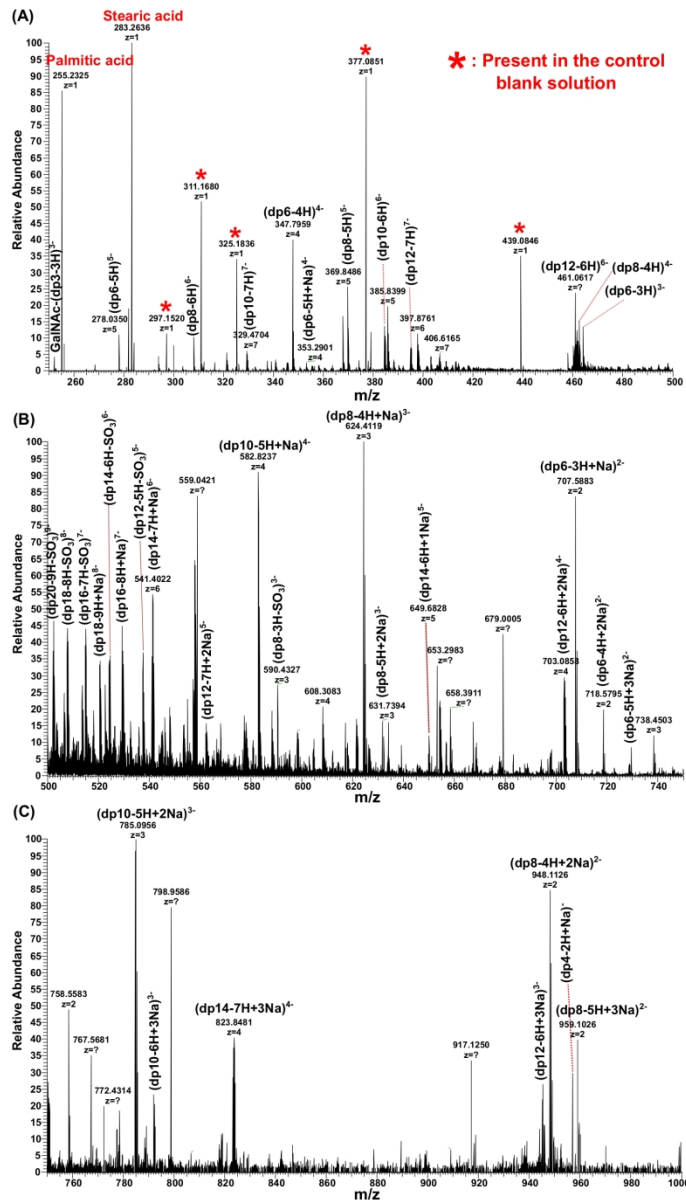
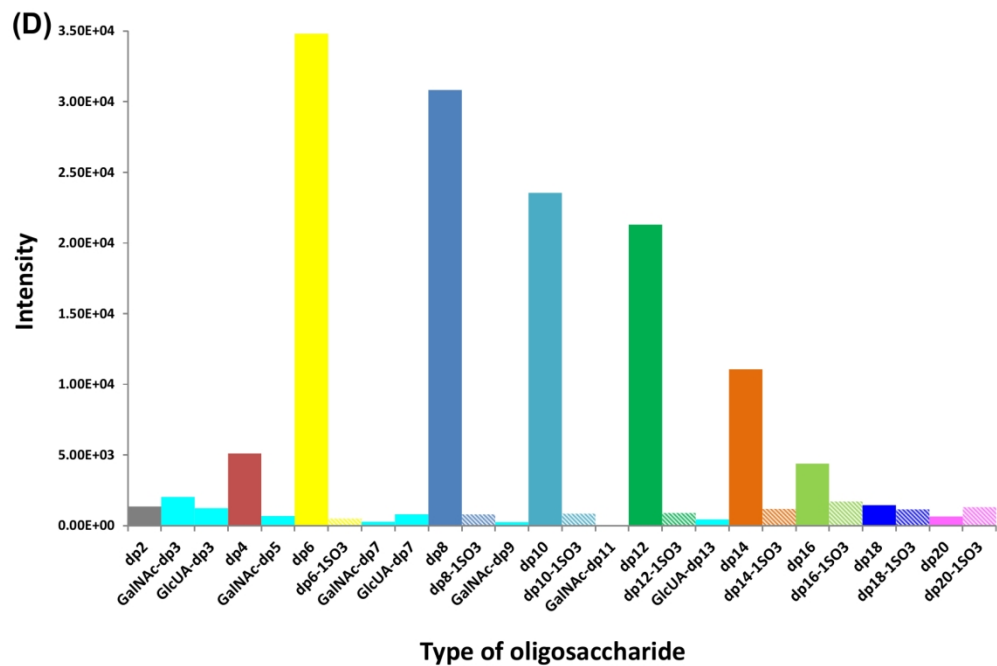


Fig. 3- Negative ion mode ESI- Orbitrap spectrum of the CS-C digest. To have a better view of the observed ions, different regions of the spectrum are shown separately as follows: (a) m/z 250-500, (b) m/z 500-750, and (c) m/z 750-1000 ranges. Ions indicated by red stars have been present in the control solution containing only the enzyme without substrate. (d) Absolute intensities of different oligosaccharides observed in the ESI-Orbitrap mass spectrum of the CS-C digest plotted according to their size, taking into account all the charge states for each oligosaccharide. For each individual ion only the intensity of the monoisotopic peak was counted. Digestion was performed by incubation of 0.2 mg of CS-C with 20 μ L of Hyal (1000 u/mL) at 37°C overnight. Direct infusion (3 μ L/min) of the digestion mixture diluted in methanol.

413x719mm (600 x 600 DPI)



476x317mm (300 x 300 DPI)

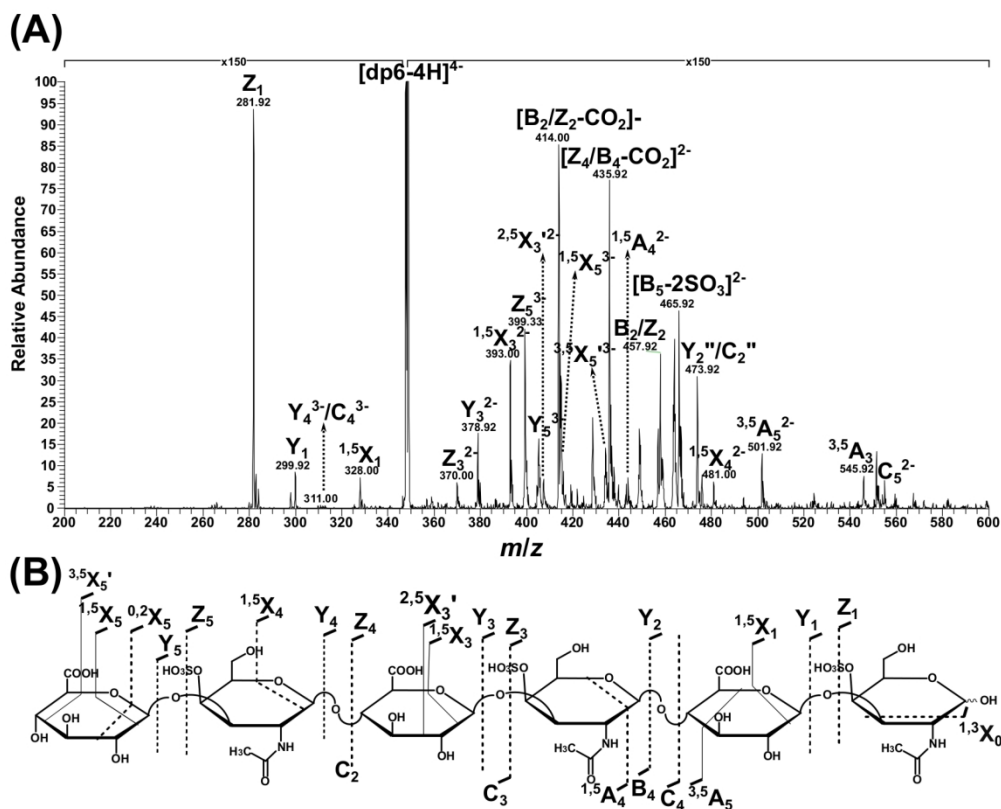


Fig. 4- Extreme-UV photodissociation of hexasaccharide SEC fraction of CS-A digestion mixture. (a) Fragmentation spectrum of the isolated ion $[dp6-4H]^{4-}$ (m/z 347.8) and (b) XUV cleavage map (without indication of the charge state of fragment ions due to space limitation). Cleavages indicated with plain lines demonstrate the sequence with a GlcUA unit at the non-reducing end (GlcUA-GalNAc(4S)-GlcUA-GalNAc(4S)). Identified fragment ions are summarized in Table S4. Digestion conditions as in Fig. 2. Direct infusion (3 μ L/min) of the digestion mixture diluted in methanol.

452x365mm (300 x 300 DPI)

